Original Paper

European Surgical Research

Eur Surg Res 2008;41:44–53
DOI: 10.1159/000128279

Received: November 19, 2007
Accepted after revision: December 11, 2007
Published online: April 28, 2008

Dose-Dependent New Bone Formation by Extracorporeal Shock Wave Application on the Intact Femur of Rabbits

T. Tischer[a, c] S. Milz[f] C. Weiler[d] C. Pautke[b] J. Hausdorf[e] C. Schmitz[g] M. Maier[e]

Departments of [a]Orthopeadic Surgery and [b]Oral and Cranio-Maxillofacial Surgery, Technical University of Munich, Departments of [c]Anatomy, [d]Pathology and [e]Orthopaedic Surgery and Institute for Surgical Research, Ludwig Maximilian University of Munich, Munich, Germany; [f]AO-Research Institute, AO Foundation, Davos, Switzerland; [g]Department of Psychiatry and Neuropsychology, Division of Cellular Neuroscience, Maastricht University, Maastricht, The Netherlands

Key Words
Animal model · New bone formation · Shock wave · Energy flux density · Histomorphometry

Abstract
Background: Whereas various molecular working mechanisms of shock waves have been demonstrated, no study has assessed in detail the influence of varying energy flux densities (EFD) on new bone formation in vivo. ***Methods:*** Thirty Chinchilla bastard rabbits were randomly assigned to 5 groups (EFD 0.0, 0.35, 0.5, 0.9 and 1.2 mJ/mm^2) and treated with extracorporeal shock waves at the distal femoral region (1,500 pulses; 1 Hz frequency). To investigate new bone formation, animals were injected with oxytetracycline at days 5–9 after shock wave application and sacrificed on day 10. Histological sections of all animals were examined using broad-band epifluorescent illumination, contact microradiography and Giemsa-Eosin staining. ***Results:*** Application of shock waves induced new bone formation beginning with 0.5 mJ/mm^2 EFD and increasing with 0.9 mJ/mm^2 and 1.2 mJ/mm^2. The latter EFD resulted in new bone formation also on the dorsal cortical bone; cortical fractures and periosteal detachment also occurred. ***Conclusion:*** Here, for the first time, a threshold level is presented for new bone formation after applying shock waves to intact bone in vivo. The findings of this study are of considerable significance for preventing unwanted side effects in new approaches in the clinical application of shock waves.

Introduction

For almost 15 years, extracorporeal shock wave therapy has been used in treatment for disorders of the musculo-skeletal system. It has been used, with varying success rates, for conditions such as tendinopathies, delayed bone healing, pseudarthrosis and aseptic femoral head necrosis [1–3]. When shock waves were found to be effective for the treatment of nonunions in 1991 [4], numerous groups investigated the effects of shock waves in animal models [5–14] and clinical-experimental applications [15–18]. Unfortunately, the application of extracorporeal shock wave therapy was not very standardized in terms of the strength and number of the impulses used, making comparisons between studies difficult. Today, the best way to characterize shock waves is the use of the energy

KARGER

Fax +41 61 306 12 34
E-Mail karger@karger.ch
www.karger.com

0014–312X/08/0411–0044$24.50/0

Accessible online at:
www.karger.com/esr

Thomas Tischer, MD
Department of Orthopaedic Surgery, Technical University of Munich
Ismaningerstrasse 22
DE–81675 Munich (Germany)
Tel. +49 89 4140 2271, Fax +49 89 4140 4849, E-Mail thomas.tischer@gmx.net

flux density (EFD; expressed in mJ/mm^2), which can be measured with laser hydrophones and accurately quantifies the applied shock wave energy, independent of the shock wave generator type or voltage setting used [19].

In recent years, the changes in molecular mechanisms induced by shock waves in tendon and bone have been partly investigated using animal and cell-culture models. Shock waves induce increased vascularization at the tendon-bone interface [20], increased collagen production and collagen cross-linking [21], and thereby promote healing of tendons. Shock waves also lead to increased biomechanical stability of tendons reattached to bone [22]. At the same time, high-energy shock waves have been shown to cause tendon damage in a dose-dependent manner [23–25]. In cell-culture experiments, cells were also damaged by high-energy shock waves [26]. At the cellular level in bone tissue, shock waves interact with numerous transmitter systems, leading to new bone formation in physiological as well as acutely fractured and pseudarthrotic bone [9, 27–35]. Involvement of growth factors like tumor growth factor (TGF-β1), various bone morphogenetic proteins (BMP) and vascular endothelial growth factor (VEGF-a), or secretion of neurotransmitter substance P has been shown. Together, the activation of underlying molecular signal cascades mediated by kinases like extracellular signal-regulated kinase (ERK), the G-protein RAS and p38 kinase have been elucidated [9, 27–35].

For the clinical application of shock waves, the mechanisms of action are very important, but the dose of the shock wave energy is also an important factor. It has been speculated by many authors that the effect of shock waves on bone (under physiologic as well as pathologic conditions) is also energy-dose dependent, but this has not been demonstrated yet. Therefore, the aim of this study was to investigate whether a dose-dependent effect of shock wave application on normal bone exists and to characterize the histological features of the newly formed bone. The results may serve as a guideline for further application of shock waves in clinical studies and could help to define a minimal energy dose that still leads to new bone formation in the rabbit model. In recent publications, remote effects of shock wave application on bone have been described. These effects include humeral head osteonecrosis, pulmonary embolism and tendon damage, particularly when high-energy shock waves with EFD over 0.9 mJ/mm^2 were used [11, 23, 36, 37]. Therefore, for the clinical application of shock waves, it is also very important to define a dose–effect relationship, in order to minimize side effects on the musculoskeletal system and improve the efficacy of this technique.

Table 1. Animal groups and physical shock wave parameters used for treatment

Group	Shock wave device	kV	EFD mJ/mm^2	Impulses n	Frequency Hz
A	EPOS	*	0.35	1,500	1
B	XL1	15	0.5	1,500	1
C	XL1	20	0.9	1,500	1
D	XL1	25	1.2	1,500	1
E	XL1	0	0	1,500	1

* The EPOS shock wave source is not adjusted using kV.

Materials and Methods

Animals

Thirty female Chinchilla bastard rabbits were investigated [exbreeders, 1 year old, body weight (BW) 4,200–4,900 g, closed femoral growth plates]. Animals were purchased from a provider of animal research models (Charles River, Kisslegg, Germany). During the experimental period, animals were maintained on a 12:12 h light:dark cycle with lights on at 6:00 a.m. and access to standard food pellets and water ad libitum. Animals were randomly assigned to 1 of 5 groups (n = 6 rabbits per group), differing with respect to the EFD of the applied extracorporeal shock waves (0.0, 0.35, 0.5, 0.9 and 1.2 mJ/mm^2; table 1). For each animal either the left or the right hindlimb was randomly selected for extracorporeal shock wave application, with the other hindlimb serving as control. All research and animal care procedures were approved by the local district government animal utilization study committee.

Anesthesia

Extracorporeal shock wave application was carried out under deep intravenous anesthesia. Anesthesia was initialized by intravenous injection of a combination of xylazine hydrochlorid (1.5 mg/kg BW) and ketamine (6 mg/kg BW) and was maintained by intravenously applying 2.4 mg/kg BW per hour xylazine hydrochlorid and 10 mg/kg BW per hour ketamine by means of a perfusion pump. During anesthesia, animals were supplied with oxygen by an oxygen mask. Administration of intravenous drugs was terminated immediately after shock wave application.

Extracorporeal Shock Wave Application

After shaving both hindlimbs, animals were positioned for extracorporeal shock wave application as previously described in detail [10]. Extracorporeal shock waves were applied to all animals as 1,500 shock wave pulses at 1 Hz frequency during 25 min. Shock waves with EFD of either 0.0 mJ/mm^2 (sham treatment), 0.5 mJ/mm^2, 0.9 mJ/mm^2 or 1.2 mJ/mm^2 (n = 6 animals per group) were applied to the distal femoral region of the selected hindlimb using an electrohydraulic shock wave source (XL1; Dornier MedTech, Wessling, Germany). The shock wave device was coupled to the selected distal femoral region by means of a water bath. Two laser pointers adjusted in 2 planes controlled focusing of the shock waves to the distal femur, the waves were directed from the

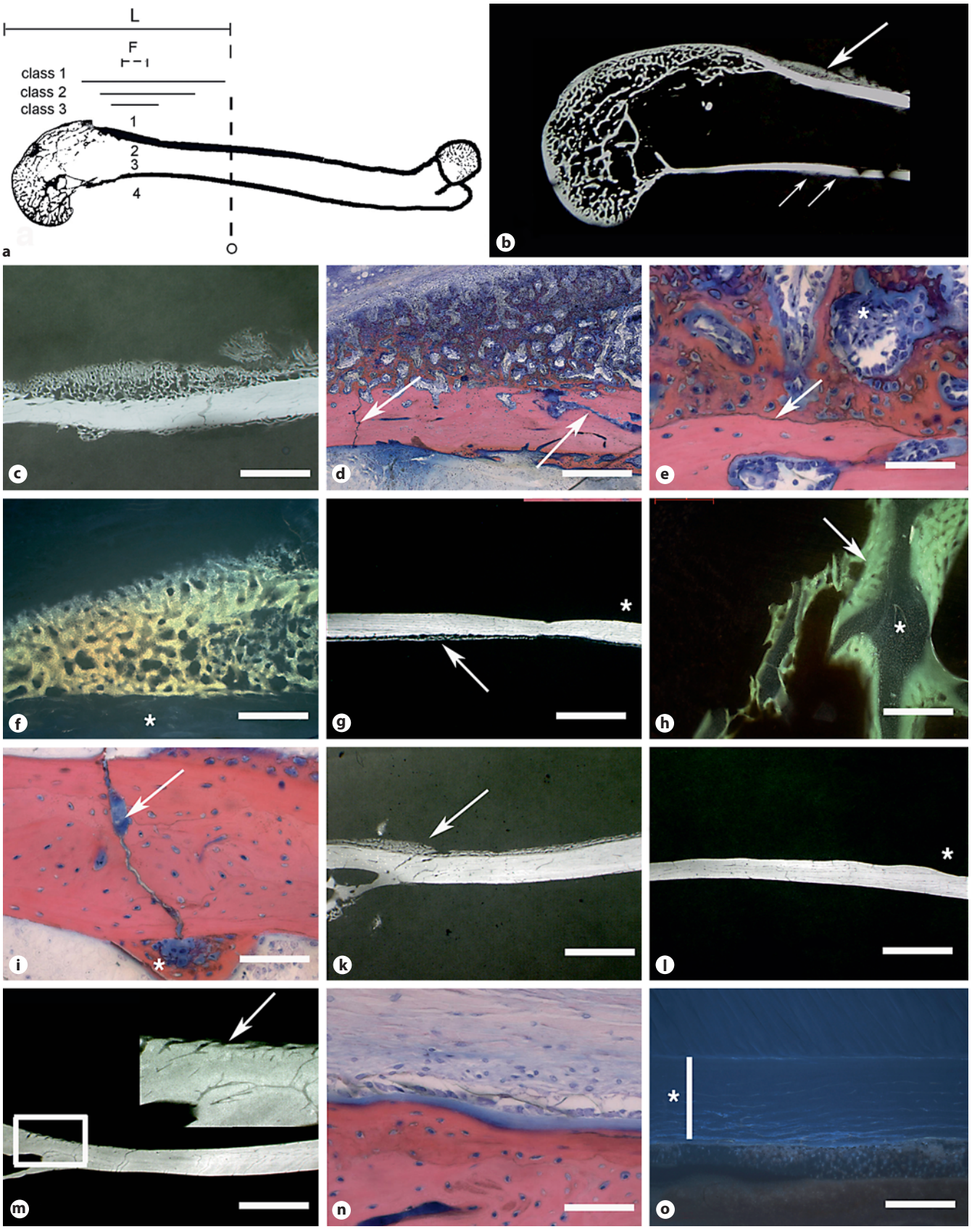
L
F
class 1
class 2
class 3
1
2
3
4
a
b
c
d
e
f
g
h
i
k
l
m
n
o

anterior femur posteriorly. In the case of sham treatment, the procedure was identical to those carried out for the treatment with 1.2 mJ/mm^2. However, the treated hindlimb was protected by a Styrofoam box that was impermeable to shock waves. Since an EFD of 0.35 mJ/mm^2 could not be generated with the electrohydraulic device, shock wave application at this EFD (n = 6 animals) was carried out with an electromagnetic shock-wave source (EPOS Ultra; Dornier MedTech, Germany). The shock wave source was coupled to the distal femoral region at the same region as with the XL-1 device (fig. 1a) by means of clinically used ultrasound jelly between application device (cylinder) and skin. Shock wave focusing to the distal femur was controlled by an outline ultrasound-system (7.5 MHz linear scan) integrated into the shock wave device.

Fig. 1. a Measurements of the rabbit femur. After sagital sections were obtained, new bone formation was measured on the periosteal-ventral (1), endosteal-ventral (2), endosteal-dorsal (3) and periosteal-dorsal (4) side. Further, the percentage of the length of new bone formation was divided into 3 classes (see text for details). L = 5 cm; F = –6 dB focus zone of shock waves. **b** Microradiography of a treated femur with EFD 1.2 mJ/mm^2. Single arrow = periosteal-ventral new bone formation; double arrow = periosteal-dorsal new bone formation. **c** Detailed view of ventral-periosteal new bone formation after ESWA with EFD 1.2 mJ/mm^2 (same specimen as shown in **b**). Scale bar = 2,000 μm. **d** Histological view of ventral cortical bone with new appositional bone formation and 2 cortical fractures filled with fibrous tissues (arrows). Giemsa-Eosin staining. Scale bar = 1,000 μm. **e** High-power image showing the border (arrow) between cortical bone and newly formed bone. Giemsa-Eosin staining. Asterisk = osteoclasts; scale bar = 250 μm. **f** High-power image showing tetracycline fluorescence labeling of the same region as shown in **c**. Cortical bone (asterisk) is unstained. Scale bar = 500 μm. **g** Microradiography shows periosteal-dorsal new bone formation after ESWA with 1.2 mJ/mm^2. Arrow = periosteal-dorsal new bone formation; asterisk = endosteal side; scale bar = 2,000 μm. **h** High-power tetracycline labeling of callus formation (arrow) in trabecular fractures in the femur condyle after ESWA with EFD 1.2 mJ/mm^2. Asterisk = unstained trabecular bone; scale bar = 250 μm. **i** High-power view of trabecular fracture (arrow) with newly formed surrounding callus (asterisk). Giemsa-Eosin staining. Scale bar = 250 μm. **k** Microradiography of periosteal-ventral new bone formation (arrow) after ESWA with 0.9 mJ/mm^2. Note that the amount of new bone formation is substantially lower than in **c**. Scale bar = 2,000 μm. **l** Dorsal cortical bone showing no periosteal-dorsal new bone formation after ESWA with EFD 0.9 mJ/mm^2. Asterisk = endosteal side; scale bar = 2,000 μm. **m** Minimal periosteal-ventral new bone formation after ESWA with EFD 0.5 mJ/mm^2 is seen in this microradiographic image. Inset shows same region as shown in **i**. There is a small irregular bone formation on the periosteal surface (arrow). Scale bar = 2,000 μm. **n** Untreated side of the animal as seen in **c**. No appositional new bone formation is seen with regular periost. Giemsa-Eosin staining. Scale bar = 250 μm. **o** High-power fluorescence-labeling image of sham-treated group showing no new bone formation. Asterisk = cortical bone; scale bar = 500 μm.

Prior to each shock wave application, the EFD of the focus zone was measured with a laser hydrophone (Imotec, Mühlanger, Germany) [11, 38, 39]. By this approach, it is possible to compare the effects of different shock wave generators (electromagnetic or electrohydraulic). The measured size of the –6 dB focus zone was 5 mm (fig. 1a). This focus zone includes all parts of the shock wave field, where the positive pressure is >50% of the peak positive pressure.

In vivo Bone Labeling

All animals received subcutaneous injections of 25 mg/kg BW oxytetracycline (5%; Atarost, Twistringen, Germany) at varying sites of the back at each of days 5–9 after extracorporeal shock wave application, modified from the protocol established by Delius et al. [5].

Analysis of Bones

Animals were sacrificed by a pentobarbital overdose 10 days after extracorporeal shock wave application. Both femurs were exarticulated in the hip and knee joint, fixed in methanol (100%) for 14 days, dehydrated and block-embedded in methylmethacrylate. Since total femur length varied only between 9.9 cm and 10.2 cm, for the further analysis each specimen was shortened to 5 cm (with a diamond band saw; Exakt, Norderstedt, Germany) for investigation of the focus zone and then cut to 100 μm-thick sagittal sections from anterior to posterior using a saw microtome (Leica SP 1600; Leitz, Wetzlar, Germany). Intervals between sections were 800 μm, and 5–7 sections were obtained from each femur. Bones were evaluated by means of broad-band epifluorescent illumination, contact microradiography and histological examination using Giemsa-Eosin staining.

Epifluorescent illumination was carried out with a microscope (Axiophot; Zeiss, Göttingen, Germany) using a fluorescent filter system (filter no. 25; Zeiss, Germany), fluorescent light source (HBO-100, Zeiss) and video camera (MC 3255P, Sony, Japan). Quantitative analysis was performed online using an image analysis system (Kontron KS 400; Zeiss). For all femurs, the following parameters were investigated at both the periosteal ventral and dorsal sites as well as at the endosteal ventral and dorsal sites: (1) maximum thickness of new bone formation measured perpendicular from the bone surface and (2) percentage of bone length showing new bone, classified into class 1 (0–33%), class 2 (34–66%) and class 3 (67–100%) (fig. 1). At the beginning of each investigation, the image analysis system was adjusted with a calibrated scale (Zeiss). The precision of the measurements was ±10 μm.

Contact microradiography was performed on high-resolution photo plates (IMTEC, Sunnyvale, Calif., USA) using a Faxitron Microfocus System (Hewlett-Packard; Palo Alto, Calif., USA) with a period of exposure of 60 min at 17 kV and 2 mA. Furthermore, sections were independently and blindly evaluated by 2 pathologists experienced with the musculoskeletal system using a Leitz Dialux 20 EB light microscope (Leitz). For all femora, the following parameters were investigated at the periosteal ventral site and the trabecular bone of the metaphysis and diaphysis: presence of periosteal new bone apposition, periosteal detachment, cortical fractures, and trabecular bone with callus. The data were scored into 3 classes. Class 1 (no sign of the investigated variables, score 1), class 2 (moderate signs of the investigated variables, score 2) and class 3 (distinct signs of the investi-

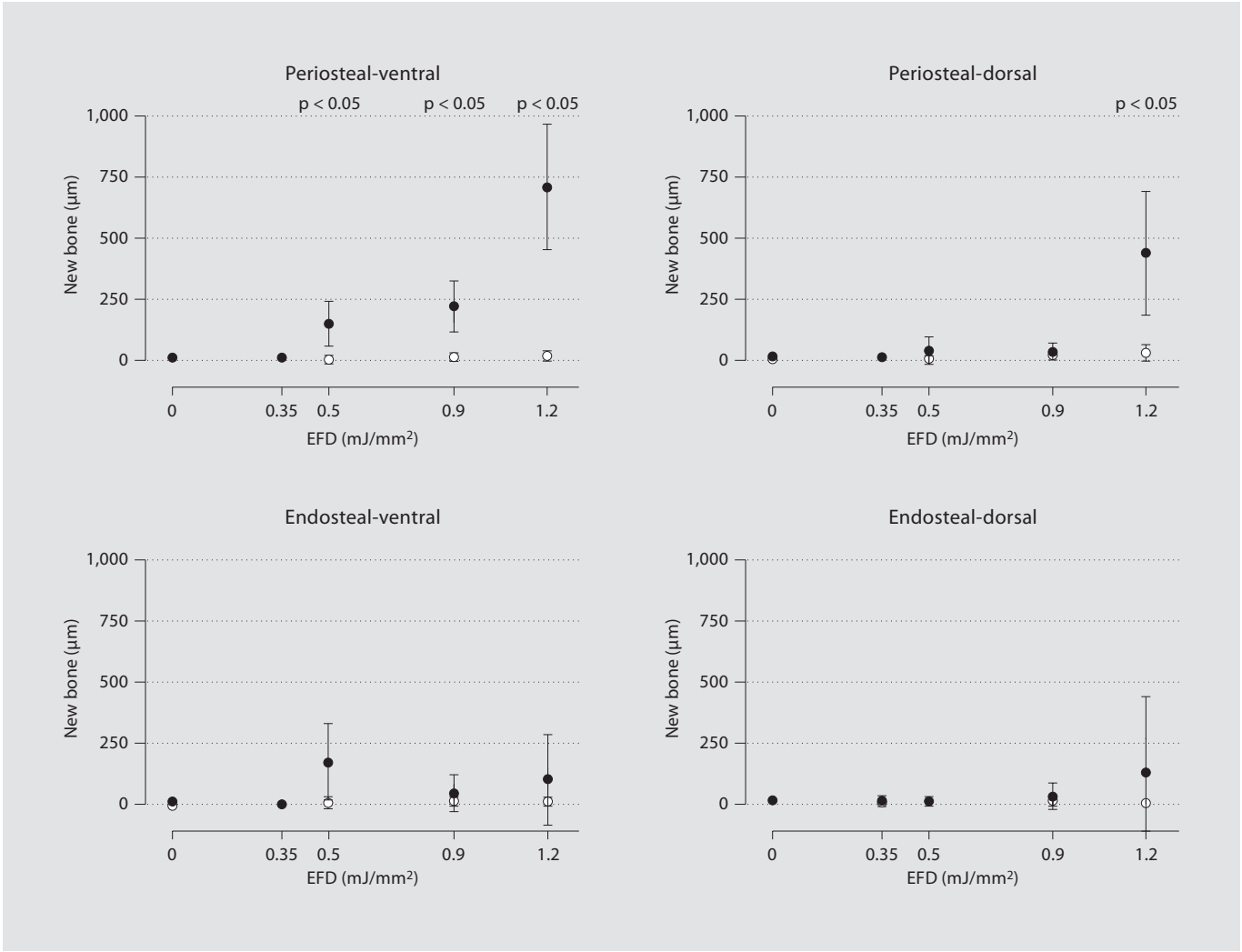

Fig. 2. Maximum new bone formation dependent on the applied EFD (0.0, 0.35, 0.5, 0.9 and 1.2 mJ/mm^2) for the periosteal ventral, periosteal dorsal, endosteal ventral and endosteal dorsal side. Data are mean ± SEM. Filled circles = treated femur; open circles = untreated femur. Statistical significance between treated and untreated femur is marked with $p < 0.05$.

gated variables, score 3). All histomorphometric gradings were assessed independently by 2 pathologists. Any differences between the classification of the 2 pathologists were resolved in conference.

After grinding and polishing (Schleifsystem 400 CS, Exakt), selected specimens were stained using Giemsa-Eosin and evaluated for signs of newly formed bone and callus formation.

Statistical Analysis

For each group of animals, the mean and standard error of the mean (SEM) were calculated for all investigated variables. Comparisons between groups (i.e., between different EFDs) were performed using nonparametric Spearman's rank correlation, separately for the treated and the untreated femora. For the investigation of the maximum thickness of new bone formation, the Wilcoxon matched pairs test was applied for comparisons within groups. In cases of extension of new bone formation, comparisons within groups (i.e., between treated and untreated femora of the same animals) were performed using χ^2 or Fisher's test, respectively. The latter test was used if one class (i.e., 1, 2 or 3) was not recorded for both the treated and the untreated femora. Differences were considered as statistically significant at $p < 0.05$. All calculations were carried out using GraphPad Prism version 4.00 for Macintosh (GraphPad Software; San Diego, Calif., USA).

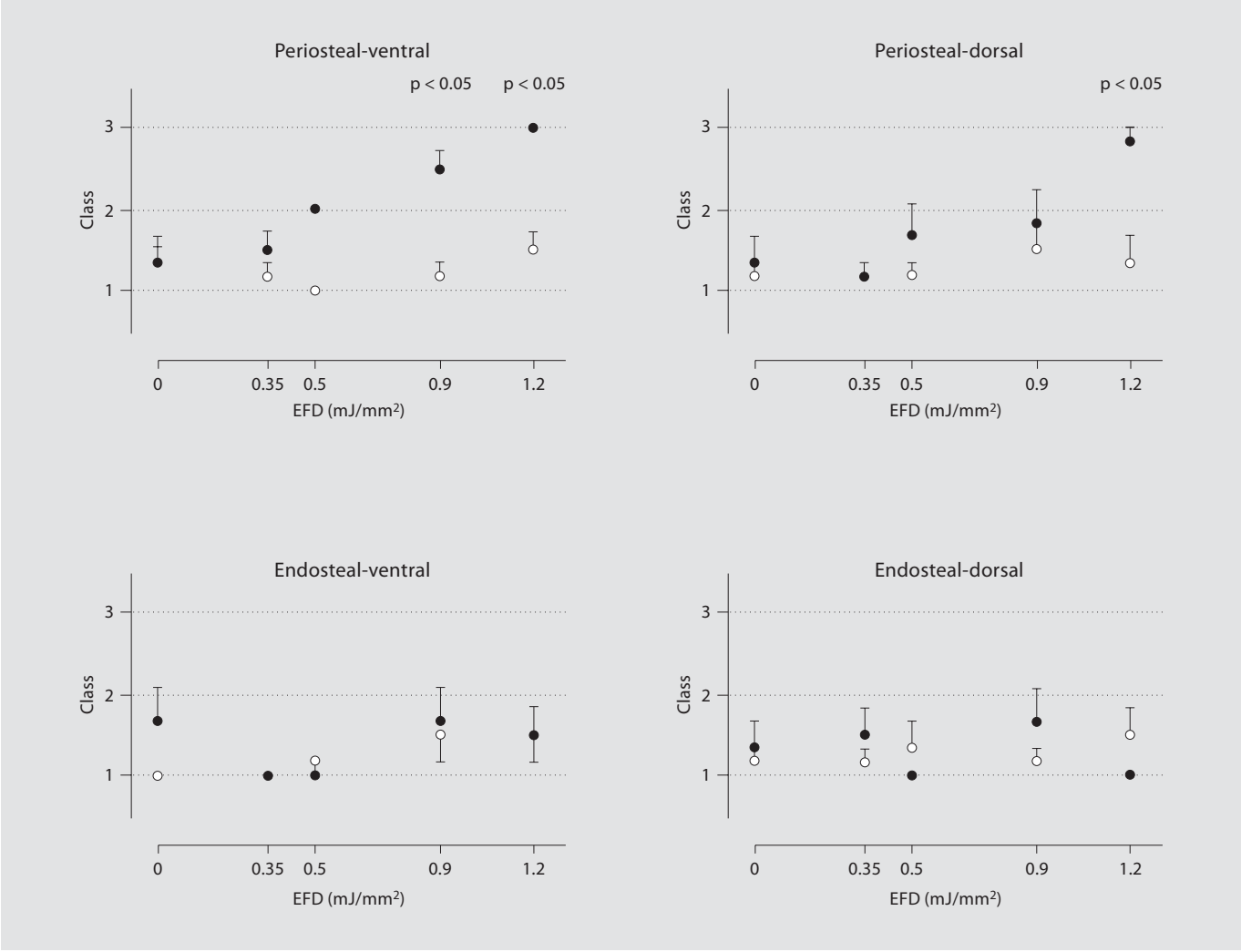

Fig. 3. Maximum length of new bone formation dependent on the applied EFD (0.0, 0.35, 0.5, 0.9 and 1.2 mJ/mm^2) for the periosteal ventral, periosteal dorseal, endostal ventral and endosteal dorsal side, classified in three groups (class 1 = 0–33%; class 2 = 34–66%; class 3 = 67–100%). Data are mean ± SEM. Filled circles = treated femur; open circles = untreated femur. Statistical significance between treated and untreated femur is marked with $p < 0.05$.

Results

Extracorporeal shock-wave application to the distal femoral region of the rabbit resulted in macroscopically detectable hematomas in the focus zone of every animal in the group treated with EFD 1.2 mJ/mm^2 and slight hematomas were detected in the animals treated with 0.9 mJ/mm^2. No hematomas were found in any other animal. Microscopically, clearly detectable, dose dependent signs of new bone formation, mostly on the periosteal-ventral side were found (fig. 1).

With respect to the investigations with epifluorescent illumination, the most distinct effects of shock wave application were found at the periosteal-ventral site of the treated femur. These effects comprised statistically significant positive correlations between the applied EFD, the maximum thickness of new bone formation and the percentage of bone length showing new bone (fig. 2 and 3). Furthermore, there were statistically significant differences between the treated and the untreated femurs of the same animals at the periosteal-ventral sites for the maximum thickness of new bone formation at EFDs of

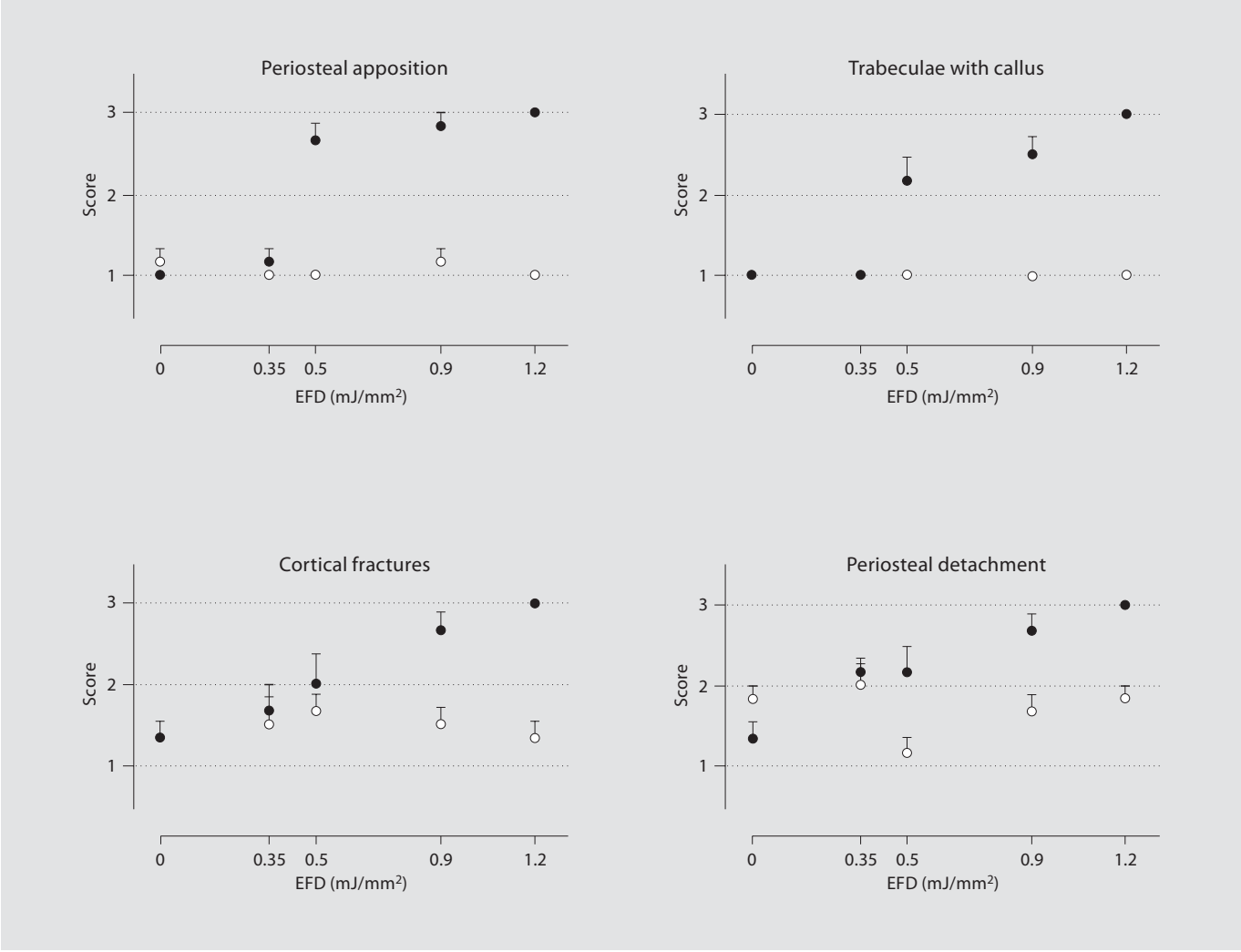

Fig. 4. Results of the contact microradiograpic analysis. New bone apposition (periosteal ventral), periosteal detachment (ventral), cortical fractures (ventral) and trabeculae with callus in the femur condyle are recorded. Values shown are mean values per group obtained from the individual classification scores (see text for details). Data are mean ± SEM. Filled circles = treated femur; open circles = untreated femur. For statistical details see text.

0.5 mJ/mm^2 (p = 0.031), 0.9 mJ/mm^2 (p = 0.031) and 1.2 mJ/mm^2 (p = 0.031) and for the percentage of total bone length showing new bone at EFDs of 0.9 mJ/mm^2 (p = 0.003) and 1.2 mJ/mm^2 (p = 0.014). Moderate effects of shock wave application were found at the periosteal dorsal site of the treated femur. However, statistical significance was only obtained for differences between the treated and the untreated femur of the same animals at EFD of 1.2 mJ/mm^2 for the maximum thickness of new bone formation periosteal-dorsal (p = 0.031) and the percentage of bone length showing new bone periosteal-dorsal (p = 0.013). At the endosteal sites of the femur, no statistically significant effects of the applied shock waves were found. All data of the investigations with epifluorescent illumination are displayed in figures 2 and 3.

The investigations with contact microradiography revealed statistically significant positive correlations in the treated femura between the applied energy flux density and periosteal new bone apposition [Spearman r (r) = 1.000, p = 0.017], periosteal detachment (r = 0.975, p = 0.017), and cortical fractures (r = 1.000, p = 0.017) at the periosteal ventral site and the trabecular bone of the me-

taphysis and diaphysis. No statistically significant correlation was found for trabecular bone with callus ($r = 0.975$, $p = 0.167$). By contrast, no correlations were found between the applied EFD and the investigated variables at the untreated femur. Furthermore, statistically significant differences between the treated and the untreated femur of the same animals were found for periosteal new bone apposition at EFDs of 0.5 mJ/mm^2 ($p = 0.003$), 0.9 mJ/mm^2 ($p = 0.007$) and 1.2 mJ/mm^2 ($p = 0.002$), periosteal detachment at EFDs of 0.9 mJ/mm^2 ($p = 0.036$) and 1.2 mJ/mm^2 ($p = 0.003$) and trabecular bone with callus at EFDs of 0.5 mJ/mm^2 ($p = 0.014$), 0.9 mJ/mm^2 ($p = 0.003$) and 1.2 mJ/mm^2 ($p = 0.002$). For cortical fractures, statistically significant differences between the treated and the untreated femur of the same animals were restricted to EFDs of 0.9 mJ/mm^2 ($p = 0.027$) and 1.2 mJ/mm^2 ($p = 0.003$), but were not observed at 0.5 mJ/mm^2 ($p = 0.264$). All data of the investigations with contact microradiography are displayed in figure 4.

Histologically, these results were confirmed. The newly formed bone was easily discerned by its cell-rich, eosinophilic matrix which showed the typical characteristics of woven bone (fig. 1e). In this area, signs of appositional bone formation were detectable with an increase in resorption lacunes with osteoclasts and a prominent layer of osteoblasts. Cortical fractures were filled with fibrous tissue (fig. 1d) and trabecular fractures showed chondrogenic and osteogenic callus tissue (fig. 1i). In contrast, the untreated femur showed no new bone formation (fig. 1n).

Discussion

The investigations were performed on an established animal model of extracorporeal shock wave application to the musculoskeletal system [5, 10]. In line with previous reports of extracorporeal shock wave therapy in animal models [5, 11, 13, 14, 40], the present study shows shock wave mediated new bone formation. In recent publications a dose-dependent effect has been assumed; however, this was based on only 1 low-dose group receiving 2,000 shock wave impulses with EFD 0.18 mJ/mm^2 and 1 high-dose group receiving 4,000 shock wave impulses with EFD of 0.47 mJ/mm^2 in a fracture model [33]. Here, a threshold value for new bone formation is presented, assessing 5 different EFD levels. Extracorporeal shock wave application resulted in a dose-dependent increase of periosteal new bone formation, requiring a minimum dose of 0.5 mJ/mm^2 to create any effect at all in this animal model. The amount of new bone formation then increased with increasing EFD (0.9 and 1.2 mJ/mm^2, $p < 0.05$).

When using a high EFD of 1.2 mJ/mm^2 new bone formation was also seen on the dorsal periosteal side of the femur. A remote action of shock waves on new bone formation has already been shown for the ventral cortical bone, but not for the dorsal cortical bone [11]. Trabecular fracturing in the femur condyle also occurred, even with lower EFD. This should be considered by the clinician when calculating possible side effects, especially when using shock waves with a relatively high EFD ($\geq$1.2 mJ/mm^2) [7]. Other serious complications, like pulmonary embolism, have been described in the same animal model also using an EFD of 1.2 mJ/mm^2 [36]. Recently, after high-energy shock wave therapy (EFD 0.78 mJ/mm^2; 3,000 impulses) for rotator cuff tendinopathy in humans, humeral head osteonecrosis was reported. There was no hint of any etiology other than the shock waves [37]. These unwanted side effects could possibly be minimized when using shock waves with an EFD just high enough to induce new bone formation (in cases of bone stimulation during fracture repair or treatment of pseudarthroses) but not so high as to induce major side effects. Furthermore, when treating soft tissue disorders like tendinopathies with shock waves, new bone formation has to be strictly avoided in order to prevent nerve entrapment syndromes, such as at the elbow or impingement syndromes at the shoulder.

Earlier explanations for shock wave-induced bone formation were based on the concept of mechanically induced microfractures and periosteal detachment [4, 5, 7]. We can here confirm that shock waves lead to cortical fractures, periosteal detachment, trabecular fractures and callus formation. According to Ikeda et al. [7], microfractures are necessary for the generation of new bone. In our study, we observed periosteal bone apposition with only minimal production of microfractures (EFD 0.5 mJ/mm^2), indicating that this might not be the prevalent mechanism for new bone formation. Similar concerns were previously raised by our group [40]. Furthermore, the release of growth factors (TGF-β1, VEGF-a and BMP) and other mediators (substance P) that affect bone formation has been shown recently in the rabbit and rat models [9, 10, 31, 35], which suggests other molecular mechanisms may have a role in the induction of new bone formation.

Despite the relatively widespread clinical use of EFD, the physical parameters for its clinical application (the dose and number of shock wave impulses), for the treatment of individual diseases still have to be standardized.

Since now a dose-dependent relationship between shock waves and biological action has been clearly proven, more clinical studies defining suitable EFD and number of shock wave impulses for single diseases have to be performed, especially since this information cannot be directly transferred to the pathological situation of fractured bone or nonunion in human bones. For example, in the treatment of tibial nonunion, Schaden et al. [17] used shock waves with an EFD of 0.4 mJ/mm^2 and 12,000 impulses and achieved union in 26 out of 34 patients. Wang et al. [18] used similar physical parameters, but with EFD a little higher and fewer impulses (EFD 0.62 mJ/mm^2; 6,000 impulses). Clinical results were similar. Finally, Rompe et al. [16] achieved healing rates of about 70% of tibial nonunions when using shock waves with EFD 0.6 mJ/mm^2 and 3,000 impulses. Other groups using different physical parameters were not as successful [15], highlighting the importance of a clearly defined energy dose for shock wave applications.

We conclude that the results presented here have significant impact on further clinical application of shock waves on bone tissue. In the present study, it is clearly demonstrated that the amount of new bone formation is directly dependent on the applied EFD. If the applied EFD is too low, no significant new bone formation will occur. If it is too high, unwanted side effects, like the formation of bone spurs in the shoulder or nerve entrapment syndromes in the elbow or feet by bony overgrowth, may result when treating tendionopathies.

Acknowledgements

We thank A. Nerlich MD, M. Delius MD, R. Putz MD, H. Korr PhD, and K. Messmer MD, for their superb help during all steps of this study. We also thank G. Adams and C. Dinter for their technical assistance. This work was supported by the Deutsche Forschungsgemeinschaft (DFG; MA 2175/2-1) and by the Friedrich-Baur Stiftung, University of Munich, Germany (0084/1999; 0094/1998).

References

1 Ogden JA, Alvarez RG, Levitt R, Marlow M: Shock wave therapy (Orthotripsy) in musculoskeletal disorders. Clin Orthop Relat Res 2001;387:22–40.
2 Ludwig J, Lauber S, Lauber HJ, Dreisilker U, Raedel R, Hotzinger H: High-energy shock wave treatment of femoral head necrosis in adults. Clin Orthop Relat Res 2001;387:119–126.
3 Wang CJ, Wang FS, Huang CC, Yang KD, Weng LH, Huang HY: Treatment for osteonecrosis of the femoral head: comparison of extracorporeal shock waves with core decompression and bone-grafting. J Bone Joint Surg Am 2005;87:2380–2387.
4 Valchanou VD, Michailov P: High energy shock waves in the treatment of delayed and nonunion of fractures. Int Orthop 1991;15:181–184.
5 Delius M, Draenert K, Al Diek Y, Draenert Y: Biological effects of shock waves: in vivo effect of high energy pulses on rabbit bone. Ultrasound Med Biol 1995;21:1219–1225.
6 Kaulesar Sukul DM, Johannes EJ, Pierik EG, van Eijck GJ, Kristelijn MJ: The effect of high energy shock waves focused on cortical bone: an in vitro study. J Surg Res 1993;54:46–51.
7 Ikeda K, Tomita K, Takayama K: Application of extracorporeal shock wave on bone: preliminary report. J Trauma 1999;47:946–950.
8 Augat P, Claes L, Suger G: In vivo effect of shock-waves on the healing of fractured bone. Clin Biomech (Bristol, Avon) 1995;10:374–378.
9 Maier M, Averbeck B, Milz S, Refior HJ, Schmitz C: Substance P and prostaglandin E2 release after shock wave application to the rabbit femur. Clin Orthop Relat Res 2003:237–245.
10 Maier M, Milz S, Tischer T, Munzing W, Manthey N, Stabler A, et al: Influence of extracorporeal shock-wave application on normal bone in an animal model in vivo. Scintigraphy, MRI and histopathology. J Bone Joint Surg Br 2002;84:592–599.
11 Tischer T, Milz S, Anetzberger H, Muller PE, Wirtz DC, Schmitz C, et al; Extracorporeal shock waves induce ventral-periosteal new bone formation out of the focus zone – results of an in-vivo animal trial (in German). Z Orthop Ihre Grenzgeb 2002;140:281–285.
12 Bischofberger AS, Ringer SK, Geyer H, Imboden I, Ueltschi G, Lischer CJ: Histomorphologic evaluation of extracorporeal shock wave therapy of the fourth metatarsal bone and the origin of the suspensory ligament in horses without lameness. Am J Vet Res 2006;67:577–582.
13 Saisu T, Kamegaya M, Wada Y, Takahashi K, Mitsuhashi S, Moriya H, et al: Acetabular augmentation induced by extracorporeal shock waves in rabbits. J Pediatr Orthop B 2005;14:162–167.
14 Takahashi K, Yamazaki M, Saisu T, Nakajima A, Shimizu S, Mitsuhashi S, et al: Gene expression for extracellular matrix proteins in shockwave-induced osteogenesis in rats. Calcif Tissue Int 2004;74:187–193.
15 Biedermann R, Martin A, Handle G, Auckenthaler T, Bach C, Krismer M: Extracorporeal shock waves in the treatment of nonunions. J Trauma 2003;54:936–942.
16 Rompe JD, Rosendahl T, Schollner C, Theis C: High-energy extracorporeal shock wave treatment of nonunions. Clin Orthop Relat Res 2001;387:102–111.
17 Schaden W, Fischer A, Sailler A: Extracorporeal shock wave therapy of nonunion or delayed osseous union. Clin Orthop Relat Res 2001;387:90–94.
18 Wang CJ, Chen HS, Chen CE, Yang KD: Treatment of nonunions of long bone fractures with shock waves. Clin Orthop Relat Res 2001;387:95–101.
19 Cleveland RO, Lifshitz DA, Connors BA, Evan AP, Willis LR, Crum LA: In vivo pressure measurements of lithotripsy shock waves in pigs. Ultrasound Med Biol 1998;24:293–306.
20 Wang CJ, Wang FS, Yang KD, Weng LH, Hsu CC, Huang CS, et al: Shock wave therapy induces neovascularization at the tendon-bone junction. A study in rabbits. J Orthop Res 2003;21:984–989.
21 Hsu RW, Hsu WH, Tai CL, Lee KF: Effect of shock-wave therapy on patellar tendinopathy in a rabbit model. J Orthop Res 2004;22:221–227.
22 Wang CJ, Wang FS, Yang KD, Weng LH, Sun YC, Yang YJ: The effect of shock wave treatment at the tendon-bone interface – an histomorphological and biomechanical study in rabbits. J Orthop Res 2005;23:274–280.

23 Maier M, Tischer T, Milz S, Weiler C, Nerlich A, Pellengahr C, et al: Dose-related effects of extracorporeal shock waves on rabbit quadriceps tendon integrity. Arch Orthop Trauma Surg 2002;122:436–441.
24 Rompe JD, Kirkpatrick CJ, Küllmer K, Schwitalle M, Krischek O: Dose-related effects of shock waves on rabbit tendo Achillis. A sonographic and histological study. J Bone Joint Surg Br 1998;80:546–552.
25 Maier M, Saisu T, Beckmann J, Delius M, Grimm F, Hupertz V, et al: Impaired tensile strength after shock-wave application in an animal model of tendon calcification. Ultrasound Med Biol 2001;27:665–671.
26 Martini L, Giavaresi G, Fini M, Borsari V, Torricelli P, Giardino R: Early effects of extracorporeal shock wave treatment on osteoblast-like cells: a comparative study between electromagnetic and electrohydraulic devices. J Trauma 2006;61:1198–1206.
27 Wang FS, Wang CJ, Huang HJ, Chung H, Chen RF, Yang KD: Physical shock wave mediates membrane hyperpolarization and Ras activation for osteogenesis in human bone marrow stromal cells. Biochem Biophys Res Commun 2001;287:648–655.
28 Wang FS, Yang KD, Chen RF, Wang CJ, Sheen-Chen SM: Extracorporeal shock wave promotes growth and differentiation of bone-marrow stromal cells towards osteoprogenitors associated with induction of TGF-beta1. J Bone Joint Surg Br 2002;84:457–461.
29 Wang FS, Wang CJ, Sheen-Chen SM, Kuo YR, Chen RF, Yang KD: Superoxide mediates shock wave induction of ERK-dependent osteogenic transcription factor (CBFA1) and mesenchymal cell differentiation toward osteoprogenitors. J Biol Chem 2002;277:10931–10937.
30 Chen YJ, Kuo YR, Yang KD, Wang CJ, Huang HC, Wang FS: Shock wave application enhances pertussis toxin protein-sensitive bone formation of segmental femoral defect in rats. J Bone Miner Res 2003;18:2169–2179.
31 Wang FS, Yang KD, Kuo YR, Wang CJ, Sheen-Chen SM, Huang HC, et al: Temporal and spatial expression of bone morphogenetic proteins in extracorporeal shock wave-promoted healing of segmental defect. Bone 2003;32:387–396.
32 Chen YJ, Kuo YR, Yang KD, Wang CJ, Sheen Chen SM, Huang HC, et al: Activation of extracellular signal-regulated kinase (ERK) and p38 kinase in shock wave-promoted bone formation of segmental defect in rats. Bone 2004;34:466–477.
33 Wang CJ, Yang KD, Wang FS, Hsu CC, Chen HH: Shock wave treatment shows dose-dependent enhancement of bone mass and bone strength after fracture of the femur. Bone 2004;34:225–230.
34 Wang FS, Wang CJ, Chen YJ, Chang PR, Huang YT, Sun YC, et al: Ras induction of superoxide activates ERK-dependent angiogenic transcription factor HIF-1alpha and VEGF-A expression in shock wave-stimulated osteoblasts. J Biol Chem 2004;279:10331–10337.
35 Chen YJ, Wurtz T, Wang CJ, Kuo YR, Yang KD, Huang HC, et al: Recruitment of mesenchymal stem cells and expression of TGF-beta 1 and VEGF in the early stage of shock wave-promoted bone regeneration of segmental defect in rats. J Orthop Res 2004;22:526–534.
36 Maier M, Freed JA, Milz S, Pellengahr C, Schmitz C: Detection of bone fragments in pulmonary vessels following extracorporeal shock wave application to the distal femur in an in-vivo animal model (in German). Z Orthop Ihre Grenzgeb 2003;141:223–226.
37 Liu HM, Chao CM, Hsieh JY, Jiang CC: Humeral head osteonecrosis after extracorporeal shock-wave treatment for rotator cuff tendinopathy. A case report. J Bone Joint Surg Am 2006;88:1353–1356.
38 Coleman AJ, Draguioti E, Tiptaf R, Shotri N, Saunders JE: Acoustic performance and clinical use of a fibreoptic hydrophone. Ultrasound Med Biol 1998;24:143–151.
39 Folberth W, Kohler G, Rohwedder A, Matura E: Pressure distribution and energy flow in the focal region of two different electromagnetic shock wave sources. J Stone Dis 1992;4:1–7.
40 Maier M, Hausdorf J, Tischer T, Milz S, Weiler C, Refior HJ, et al: New bone formation by extracorporeal shock waves. Dependence of induction on energy flux density (in German). Orthopade 2004;33:1401–1410.